PHILOSOPHICAL TRANSACTIONS OF THE ROYAL SOCIETY A MATHEMATICAL, PHYSICAL & ENGINEERING SCIENCES

Acoustic Scattering by a Finite Elastic Strip

J. F. M. Scott

Phil. Trans. R. Soc. Lond. A 1992 **338**, 145-167
doi: 10.1098/rsta.1992.0006

Acoustic scattering by a finite elastic strip

By J. F. M. Scott

Topexpress Limited, Poseidon House, Castle Park, Cambridge CB3 0RD, U.K.

Contents

A method for exact reduction of finite Wiener–Hopf type diffraction problems to an infinite set of simultaneous equations is presented. The problem considered is that of acoustic scattering by a finite elastic strip. The numerical implementation of the method is described and the truncation of the infinite set of equations is shown to converge to the full solution as the number of equations and unknowns goes to infinity. Results of the numerical computations are given and show effects of the leaky wave above the coincidence frequency of the plate and resonances below that frequency.

1. Introduction

The treatment of wave diffraction from semi-infinite scatterers using the Wiener–Hopf technique is well established (see, for example, Noble 1958) and has proved highly successful in a wide class of problems. In contrast, the analysis of scattering from finite objects remains less developed and it is to one specific problem in this area that we devote this paper.

A different class of scattering problems can be solved by separation of variables (see, for example, Morse & Feshbach 1953). Such problems include spherical and cylindrical scatterers and also ellipsoids and strips if the boundary conditions permit.

The extension of the Wiener–Hopf technique to finite scatterers has been the subject of some study (see, for example, Noble 1958, §5.6; Keogh 1985; Gautsen 1988*a*, *b*). These authors develop asymptotic expansions in the limit of large, but finite scatterers.

Phil. Trans. R. Soc. Lond. A (1992) **338**, 145–167
Printed in Great Britain

Application of the Wiener–Hopf technique to semi-infinite problems leads to their solution in closed form, sometimes with a set of simultaneous equations to solve for unknown constants. For finite strips or cylinders, the result of applying the technique is a pair of coupled integral equations (see Noble 1958). This is the aspect of such problems which makes their exact analysis difficult. The central component of our work is that a certain unknown function of complex wavenumber, which satisfies an integral equation, is expanded as a power series in a known function of wavenumber (the latter function being a Moebius transform). The coefficients of the power series form an infinite set of unknowns and it turns out that the integral equation can be reduced to a set of simultaneous equations for the coefficients.

The specific problem I have chosen to study is the scattering of an acoustic plane wave by a finite elastic strip. The semi-infinite equivalent of this problem has been examined by Cannell (1975, 1976) and Crighton & Innes (1984).

The analysis of the finite strip proceeds as follows. Half-range Fourier transforms are defined at each end of the strip as if the strip was semi-infinite. Since it is in fact finite, the resulting Wiener–Hopf equation for each end contains a term resulting from the transform over the extension of the strip at the other end. Formal solution of the Wiener–Hopf equations results in the integral equations referred to above.

Section 2 describes both the formulation of the problem and the subsequent analysis needed to produce the Wiener–Hopf equations. In §3 we derive the associated integral equations. Section 4 is devoted to an approximation which is obtained by neglecting certain terms that are formally small in the limit of wide strips. This procedure reproduces the results which would be obtained if the edges of the strip were regarded as semi-infinite, coupled only through the modes of propagation allowed on an infinite fluid-loaded plate (an informal method that has, for instance, been used by Crighton & Innes (1984) when treating the finite, but long version of the present problem in the limit of heavy fluid loading and also by Abrahams (1981) for the baffled strip, again in the limit of heavy loading). This approximation provides a simpler physical interpretation than the analysis of the full finite problem which we describe in §5.

Numerical implementation of the procedure for a finite strip is discussed in Appendixes A–C. This mostly involves the numerical evaluation of various complex contour integrals. The emphasis here is on a suitable choice of contour, the removal of poles which lie near that contour and the reduction to a finite domain of integration via a transformation of integration variable. Once this is achieved the numerical evaluation of integrals of smooth functions on finite intervals is straightforward.

The numerical solution of the infinite set of simultaneous equations resulting from our analysis is achieved by truncation of the equations to a finite number. It is shown in Appendix D that the solution of these finite problems approaches the solution of the infinite problem as the number of equations (and unknowns) increases.

Finally, a discussion and some results of the method are given in §6. These show resonant behaviour below the coincidence frequency of the plate, a topic which has been examined in the light-fluid-loading limit by Leppington (1976) and in the heavy loading limit by Abrahams (1981).

PHILOSOPHICAL TRANSACTIONS OF THE ROYAL SOCIETY A MATHEMATICAL, PHYSICAL & ENGINEERING SCIENCES

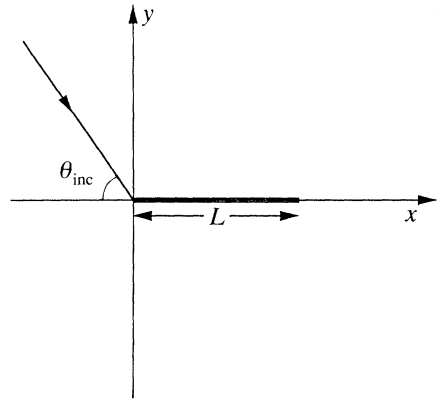

Figure 1. Scattering by a finite strip showing the coordinate system.

2. Derivation of the Wiener–Hopf equation

The semi-infinite version of our problem was studied by previous authors. We therefore keep the description as brief as possible. Our formulation is, I believe, simpler than those previously presented. It is also intended to be symmetric in relation to the two edges.

A thin elastic plate occupies the strip $0 < x < L$, $y = 0$ and is irradiated by a plane acoustic wave for which the pressure is

$$p_{\text{inc}} = \exp\{\mathrm{i}k_{\text{inc}}\, x + \gamma_{\text{inc}}\, y - \mathrm{i}\omega t\}, \tag{2.1}$$

where

$$k_{\text{inc}} = k_0 \cos\theta_{\text{inc}}, \quad \gamma_{\text{inc}} = -\mathrm{i}k_0 \sin\theta_{\text{inc}}, \tag{2.2}$$

and $k_0 = \omega/c$ is the acoustic wavenumber. Henceforth we suppress the explicit time dependence. The geometry is shown in figure 1. We note that, although the fluid surrounds the elastic strip, occupying both the region $y < 0$ and $y > 0$, we shall restrict attention to the half-space $y > 0$. This is possible because the scattered pressure, $\psi = p - p_{\text{inc}}$, is antisymmetric under reflection in the plane $y = 0$.

The scattered pressure satisfies the conditions

$$\psi = 0; \quad y = 0, \ x < 0 \ \text{ or } \ x > L, \tag{2.3}$$

and for a plate displacement η, the motion of the plate is governed by

$$B(\partial^4\eta/\partial x^4 - k_{\text{p}}^4\,\eta) + 2\psi = 0; \quad y = 0+, \ 0 < x < L. \tag{2.4}$$

The kinematic condition is given by

$$\partial p/\partial y = \rho_0\,\omega^2\eta; \quad y = 0+, \ 0 < x < L. \tag{2.5}$$

In (2.4) and (2.5), B is bending stiffness, k_{p} is the plate wavenumber in the absence of fluid loading ($k_{\text{p}}^4 = m\omega^2/B$, m being mass per unit area of plate) and ρ_0 is ambient fluid density. Finally, ψ, satisfies the Helmholtz equation

$$\partial^2\psi/\partial x^2 + \partial^2\psi/\partial y^2 + k_0^2\,\psi = 0 \tag{2.6}$$

in the fluid region exterior to the plate.

I adopt the conventional ploy of introducing some artificial dissipation in the fluid by making the acoustic wavenumber slightly complex, i.e. $k_0 = \omega/c + \mathrm{i}\epsilon$ with $\epsilon > 0$. This has the effect of making the scattered wave, ψ, exponentially decaying, as $\mathrm{e}^{-\epsilon r}$,

for large distances r from the plate, resulting in strips of analyticity when we take Fourier transforms. For instance the full-range transform

$$\tilde{\psi}(k) = \int_{-\infty}^{\infty} \psi \, \mathrm{e}^{\mathrm{i}kx} \, \mathrm{d}x \tag{2.7}$$

is an analytic function of complex k within the strip D defined by $|\mathrm{Im}\,(k)| < \epsilon$. Taking a full-range transform of (2.6) and solving for $\tilde{\psi}$ subject to the radiation condition of exponential decay at large distances yields

$$\partial\tilde{\psi}/\partial y = -\gamma\tilde{\psi}\,; \quad y = 0+, \tag{2.8}$$

where γ is the usual acoustic square root $\gamma = (k^2 - k_0^2)^{\frac{1}{2}}$ defined in the strip D to have positive real part. Extension of γ to all complex k leads to branch cuts from $k = \pm k_0$ which do not enter D, but instead go upwards or downwards from their branch points along paths which are arbitrary at this stage.

Equations (2.3)–(2.5) and (2.8) together with the edge conditions of the plate describe the problem. If we were solving the semi-infinite problem we would define half-range transforms relative to the edge of the plate. Here we have two edges, at $x = 0$ and L, and it is natural to define two pairs of half-range transforms. Thus

$$\psi_+^{(0)}(k) = \int_0^{\infty} \psi(y = 0+) \, \mathrm{e}^{\mathrm{i}kx} \, \mathrm{d}x, \tag{2.9}$$

$$\psi_-^{(0)}(k) = \int_{-\infty}^{0} \psi(y = 0+) \, \mathrm{e}^{\mathrm{i}kx} \, \mathrm{d}x \tag{2.10}$$

refer to the edge at $x = 0$ and

$$\psi_+^{(L)}(k) = \int_{-\infty}^{L} \psi(y = 0+) \, \mathrm{e}^{\mathrm{i}k(L-x)} \, \mathrm{d}x, \tag{2.11}$$

$$\psi_-^{(L)}(k) = \int_{L}^{\infty} \psi(y = 0+) \, \mathrm{e}^{\mathrm{i}k(L-x)} \, \mathrm{d}x \tag{2.12}$$

to that at $x = L$. We also write $\psi_\pm'^{(0)}$ and $\psi_\pm'^{(L)}$ for the corresponding transforms of $\partial\psi/\partial y$. The quantities with subscript '+' are analytic in the half-plane D_+, defined by $\mathrm{Im}\,(k) > -\epsilon$, while those with subscript '−' are analytic in $D_-(\mathrm{Im}\,(k) < \epsilon)$.

It is clear that the above transforms, which are defined in overlapping sections of the x-axis, are not independent of each other. Thus the full-range transform $\tilde{\psi}(y = 0+)$ can be related to the half-range transforms via

$$\tilde{\psi}(k) = \psi_+^{(0)}(k) + \psi_-^{(0)}(k), \tag{2.13}$$

or

$$\tilde{\psi}(k) = \mathrm{e}^{\mathrm{i}kL}(\psi_+^{(L)}(-k) + \psi_-^{(L)}(-k)). \tag{2.14}$$

In addition, we can also define a finite range transform

$$\bar{\psi}(k) = \int_0^{L} \psi(y = 0+) \, \mathrm{e}^{\mathrm{i}kx} \, \mathrm{d}x, \tag{2.15}$$

which is analytic for all complex k and can be related to the previous definitions via

$$\tilde{\psi}(k) = \bar{\psi}(k) + \psi_-^{(0)}(k) + \mathrm{e}^{\mathrm{i}kL}\,\psi_-^{(L)}(-k) \tag{2.16}$$

for k in D.

Taking finite range transforms of (2.4) and (2.5) yields

$$\tfrac{1}{2}B(k^4-k_{\rm p}^4)\,\bar{\eta}+\bar{\psi}=Q^{(0)}(k)+\mathrm{e}^{\mathrm{i}kL}\,Q^{(L)}(-k) \tag{2.17}$$

and

$$\bar{\psi}'=\rho_0\,\omega^2\bar{\eta}+[\mathrm{i}\gamma_{\rm inc}/(k+k_{\rm inc})]\{\exp[\mathrm{i}(k+k_{\rm inc})\,L]-1\}, \tag{2.18}$$

where $\bar{\eta}$ and $\bar{\psi}'$ are the finite-range transforms of η and $\partial\psi/\partial y$ respectively and we have used (2.1) to write $\partial p/\partial y$ in terms of $\partial\psi/\partial y$. The quantities $Q^{(0)}$ and $Q^{(L)}$ are the edge polynomials which are associated with plate edges and arise when taking finite Fourier transforms of the plate equation. They are given by

$$Q^{(0)}(k)=\tfrac{1}{2}B\{\mathrm{i}\eta_0\,k^3-\eta_0'\,k^2-\mathrm{i}\eta_0''\,k+\eta_0'''\} \tag{2.19}$$

and

$$Q^{(L)}(k)=\tfrac{1}{2}B\{\mathrm{i}\eta_L\,k^3+\eta_L'\,k^2-\mathrm{i}\eta_L''\,k-\eta_L'''\}, \tag{2.20}$$

where η_0, η_0', η_0'' and η_0''' refer to the values of η and its x-derivatives at the edge $x=0$, while η_L, etc., refer to the other edge. We note that there are two plate boundary conditions to be satisfied at each edge (e.g. $\eta''=\eta'''=0$ at a free edge, $\eta=\eta'=0$ at a clamped edge, $\eta=\eta''=0$ at a pinned edge) and this leaves two implicit unknowns in each of $Q^{(0)}$ and $Q^{(L)}$ to be determined later.

From (2.8) we have

$$\bar{\psi}'+\psi_-'^{(0)}(k)+\mathrm{e}^{\mathrm{i}kL}\,\psi_-'^{(L)}(-k)=-\gamma\tilde{\psi}, \tag{2.21}$$

while from (2.3)

$$\bar{\psi}=\tilde{\psi}.$$

These two equations can be used to eliminate $\bar{\psi}$ and $\bar{\psi}'$ from (2.17) and (2.18) which can then be combined by elimination of $\bar{\eta}$ to give

$$K(k)\,\tilde{\psi}(k)=\Lambda^{(0)}(k)+\mathrm{e}^{\mathrm{i}kL}\,\Lambda^{(L)}(-k) \tag{2.23}$$

for k in D, where $\Lambda^{(0)}$ and $\Lambda^{(L)}$ are defined below, while

$$K(k)=1-\gamma P(k) \tag{2.24}$$

and the polynomial P is

$$P(k)=(B/2\rho_0\,\omega^2)\,(k^4-k_{\rm p}^4). \tag{2.25}$$

The function $K(k)$ will turn out to be the Wiener–Hopf kernel.

The zeros of $K(k)$ give the wavenumbers of the free modes of propagation on an infinite fluid-loaded plate. The corresponding modes of the plate without fluid loading are described by the zeros of $P(k)$.

The functions $\Lambda^{(0)}$ and $\Lambda^{(L)}$ are important in our analysis and are given by

$$\Lambda^{(*)}(k)=Q^{(*)}(k)+P(k)\,\{\psi_-'^{(*)}(k)-a^{(*)}/(k+k_{\rm inc}^{(*)})\} \tag{2.26}$$

for k in D_-, where here and elsewhere the dummy index * may take the values 0 or L. The quantities $a^{(*)}$ and $k_{\rm inc}^{(*)}$ occurring in (2.26) are defined as follows. Let $A^{(0)}=1$ and $A^{(L)}=\mathrm{e}^{\mathrm{i}k_{\rm inc}L}$ be the incident wave amplitudes as seen by the edges at 0 and L respectively. Further, let $\theta_{\rm inc}^{(0)}=\theta_{\rm inc}$ and $\theta_{\rm inc}^{(L)}=\pi-\theta_{\rm inc}$ be the angles of incidence with respect to the corresponding edges. We then define $a^{(*)}=\mathrm{i}\gamma_{\rm inc}A^{(*)}$ and $k_{\rm inc}^{(*)}=k_0\cos\theta_{\rm inc}^{(*)}$. Thus $k_{\rm inc}^{(0)}=k_{\rm inc}=-k_{\rm inc}^{(L)}$.

Equation (2.23) may easily be turned into Wiener–Hopf equations for both edges. For $x=0$ we simply use $\tilde{\psi}=\psi_+^{(0)}$, while for $x=L$ we use $\tilde{\psi}=\mathrm{e}^{\mathrm{i}kL}\,\psi_+^{(L)}(-k)$ and the symmetry $K(-k)=K(k)$. Thus

$$K(k)\,\psi_+^{(*)}(k)=\Lambda^{(*)}(k)+\mathrm{e}^{\mathrm{i}kL}\,G^{(*)}(k), \tag{2.27}$$

where

$$G^{(0)}(k)=\Lambda^{(L)}(-k),\quad G^{(L)}(k)=\Lambda^{(0)}(-k). \tag{2.28}$$

Equation (2.27) gives the Wiener–Hopf equation for both edges.

The usual Wiener–Hopf equation is of the form (2.27) with $A^{(*)}$ analytic in D_-. In fact, from (2.26), we see that $A^{(*)}$ is analytic in D_- except for a single pole of known residue at $k = -k^{(*)}_{\mathrm{inc}}$. This pole provides no great obstacle to the Wiener–Hopf argument.

If the term $\mathrm{e}^{\mathrm{i}kL}G^{(*)}$ is omitted from (2.27), we recover the equation for the semi-infinite problem. This term therefore represents the effects of the other end of the strip, i.e. waves which are scattered from the other end and which impinge on the edge at $x = *$.

In addition to the Wiener–Hopf equation (2.27), whose formal solution we derive in the next section, a number of conditions are needed to ensure that all half or finite range transforms are analytic in appropriate domains. Now although $A^{(*)}(k)$ is defined by (2.26) only for k in D_-, when we have solved the Wiener–Hopf problem, we will have expressions for it which are valid for all complex k. We can already see that (2.22) and (2.23) provide an extension of $A^{(*)}(k)$ to D_+ because $\bar{\psi}$ is analytic everywhere. Evaluating (2.17) at a root of $P(k) = 0$ and using (2.22)–(2.24) we have

$$A^{(0)}(k) - Q^{(0)}(k) = -\mathrm{e}^{\mathrm{i}kL}\{A^{(L)}(-k) - Q^{(L)}(-k)\}, \tag{2.29}$$

which holds at all roots of $P = 0$.

Now for a root of $P = 0$ in D_- equation (2.26) yields

$$A^{(*)}(k) = Q^{(*)}(k), \tag{2.30}$$

which can be combined with (2.29) to show that in fact (2.30) hold at *all* roots of $P(k) = 0$ even those not in D_-. Equation (2.30) evaluated at each of the four roots of $P = 0$ give the conditions necessary for analyticity of all functions in their respective domains. These conditions will allow us to solve for all unknowns, including those implicit in $Q^{(*)}$.

Finally, we should note that (2.23), written in the form

$$\tilde{\psi}(k) = (A^{(0)}(k) + \mathrm{e}^{\mathrm{i}kL}A^{(L)}(-k))/K(k) \tag{2.31}$$

gives the Fourier transform of the scattered field from which the scattered pressure at any point can be obtained from

$$\psi = \frac{\mathrm{sgn}\,(y)}{2\pi}\int_{-\infty}^{\infty}\tilde{\psi}(k)\,\mathrm{e}^{\mathrm{i}kx-\gamma|y|}\,\mathrm{d}k \tag{2.32}$$

if required. Of course, the functions $A^{(*)}(k)$ occurring in (2.31) remain to be determined and this is the objective of what follows.

3. Formal solution of the Wiener–Hopf problem

In all applications of the Wiener–Hopf technique, a product split of the kernel is required. Thus $K = K_+K_-$ with $K_\pm$ analytic and non-zero in $\hat{D}_\pm$, where the domains $\hat{D}_\pm$ are upper and lower halves of the complex plane which overlap in a strip $\hat{D}$. When dissipation in the fluid is set to zero it is known (see, for example, Crighton 1979) that there is only one pair of real zeros of $K(k)$ (which have the form $k = \pm\hat{k}$ with $\hat{k} > k_0$). For small positive ϵ, the positive root moves into the domain $\mathrm{Im}(\hat{k}) > 0$ so that the mode in question is attenuated as it propagates. Let $\iota = \min(\epsilon, \mathrm{Im}(\hat{k}))$ so that $K(k)$ has no zeros in the new strip $\hat{D}$ defined by $|\mathrm{Im}\,(k)| < \iota$. The strip $\hat{D}$ is contained inside

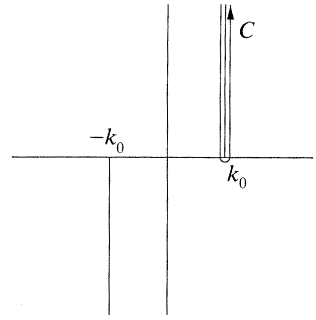

Figure 2. Complex k-plane showing the integration contour, C, and branch cuts for γ.

the strip D which was defined in §2. The standard product split $K(k) = K_+(k)\,K_-(k)$, with the normalization $K_+(k) = K_-(-k)$ can now be used (see, for example, Noble 1958). When extended to all complex k, $K_+(k)$ is analytic apart from the branch cut for γ emanating from $k = -k_0$ and non-zero except for those roots of $K(k) = 0$ which lie in $\hat{D}_-$. The large k asymptotics of K_+ are $K_+(k) \sim \text{const.} \times k^{\frac{5}{2}}$.

If, as usual, we divide the Wiener–Hopf equation (2.27) by $K_-(k)$ we have a function on the left which is analytic in $\hat{D}_+$ and the first term on the right is analytic in $\hat{D}_-$ apart possibly from a pole at $k = -k_{\text{inc}}^{(*)}$. The remaining term is

$$H^{(*)}(k) = \mathrm{e}^{\mathrm{i}kL}\,G^{(*)}(k)/K_-(k) \tag{3.1}$$

of which we wish to form the additive split $H^{(*)}(k) = H_+^{(*)}(k) + H_-^{(*)}(k)$.

The function $G^{(*)}$ is given by (2.28) and is analytic in D_+ except for a pole at $k = -k_{\text{inc}}^{(*)}$. It follows that in D_+, $H^{(*)}$ has the following singularities: the branch-cut for γ and poles at all roots of $K_-(k)$ plus a pole at $k = -k_{\text{inc}}^{(*)}$. We denote the roots of $K(k) = 0$ in $\hat{D}_+$ by $k = \hat{k}_n$ $(n = 1, \ldots, N)$. These roots are the mode wavenumbers of the infinite fluid-loaded plate.

Let us define $H_-^{(*)}$ by

$$H_-^{(*)} = \sum_{n=1}^{N} \frac{\hat{a}_n^{(*)}}{k - \hat{k}_n} - \Omega_-^{(*)}(k), \tag{3.2}$$

where

$$\hat{a}_n^{(*)} = \mathrm{e}^{\mathrm{i}\hat{k}_n L}\,G^{(*)}(\hat{k}_n)/K_-'(\hat{k}_n) \tag{3.3}$$

with $K_-' = \mathrm{d}K_-/\mathrm{d}k$ and

$$\Omega_-^{(*)}(k) = \frac{(k_0 + k)^2}{2\pi\mathrm{i}} \int_C \frac{\mathrm{e}^{\mathrm{i}sL}\,G^{(*)}(s)}{(k_0 + s)^2\,(s - k)\,K_-(s)}\,\mathrm{d}s. \tag{3.4}$$

In this integral the contour of integration, C, lies in D_+ and runs around the branch-cut for γ: down the left-hand side, around the branch point at $s = k_0$ and up the right-hand side of the cut as shown in figure 2. The contour should not enclose the points $s = k$, $s = -k_{\text{inc}}^{(*)}$ and $s = \hat{k}_n$ but is otherwise arbitrary.

The function $\Omega_-^{(*)}$ is analytic throughout the complex k-plane except for the branch-cut for γ emanating from $k = k_0$. At the branch-cut it undergoes the same jump in value as $-H^{(*)}$. The function $H_-^{(*)}$ is analytic in $\hat{D}_-$, while in D_+, it inherits the poles of $H^{(*)}$ with the correct residues by virtue of (3.3). It now follows that if we define $H_+^{(*)} = H^{(*)} - H_-^{(*)}$ then $H_+^{(*)}$ is analytic in D_+ apart from a pole at $k = -k_{\text{inc}}^{(*)}$.

Let us define

$$f_+^{(*)}(k) = K_+\,\psi_+^{(*)} + b^{(*)}/(k + k_{\text{inc}}^{(*)}) - H_+^{(*)} \tag{3.5}$$

and $$f_-^{(*)}(k) = \Lambda^{(*)}/K_- + b^{(*)}/(k+k_{\rm inc}^{(*)}) + H_-^{(*)}, \tag{3.6}$$

where $$b^{(*)} = P(k_{\rm inc}^{(*)})\, a^{(*)}/K_-(-k_{\rm inc}^{(*)}), \tag{3.7}$$

so that the Wiener–Hopf equation (2.27) yields $f_+^{(*)} = f_-^{(*)}$ in D.

From (2.26) we see that the pole of (3.6) at $k = -k_{\rm inc}^{(*)}$ has zero residue by virtue of (3.7). It follows that $f_-^{(*)}$ is analytic in $\hat{D}_-$. Equation (3.5) defines $f_+^{(*)}$ as analytic in D_+, aside from a potential pole at $k = -k_{\rm inc}^{(*)}$. Now we have already seen that $f_-^{(*)}$ has no pole at $k = -k_{\rm inc}^{(*)}$ and that $f_+^{(*)} = f_-^{(*)}$ throughout D. Thus $f_+^{(*)}$ is in fact analytic in D_+. Following the Wiener–Hopf argument, $f_\pm^{(*)}$ define an entire function of complex k. It now remains to consider the behaviour of $f_\pm^{(*)}$ as $k \to \infty$.

The usual results concerning the behaviour of half-range transforms at large k (see Noble 1958) yield $\psi_+^{(*)} = O(k^{-1})$ in D_+ and $\psi_-'^{(*)} = O(k^{-\frac{1}{2}})$ in D_-. It may then be shown that $f_+^{(*)} = O(k^{\frac{3}{2}})$ and $f_-^{(*)} = O(k)$ as $k \to \infty$ in D_+ and D_- respectively. The extended form of Liouville's theorem therefore leads to

$$f_+^{(*)} = f_-^{(*)} = E_0^{(*)} + E_1^{(*)}(k_0 - k), \tag{3.8}$$

where $E_0^{(*)}$ and $E_1^{(*)}$ are unknown coefficients.

From (3.2), (3.6) and (3.8) we have finally

$$\Lambda^{(*)} = K_-(k)\{E_0^{(*)} + E_1^{(*)}(k_0 - k) - \frac{b^{(*)}}{k+k_{\rm inc}^{(*)}} + \sum_{n=1}^{N} \frac{\hat{a}_n^{(*)}}{\hat{k}_n - k} + \Omega_-^{(*)}(k)\}, \tag{3.9}$$

which gives the formal solution of the Wiener–Hopf problem with $\hat{a}_n^{(*)}$ and $\Omega_-^{(*)}$ obtained from (2.28), (3.3) and (3.4) as

$$\hat{a}_n^{(0)} = \mathrm{e}^{\mathrm{i}\hat{k}_n L}\, \Lambda^{(L)}(-\hat{k}_n)/K_-'(\hat{k}_n) \tag{3.10}$$

and $$\Omega_-^{(0)}(k) = \frac{(k_0+k)^2}{2\pi\mathrm{i}} \int_C \frac{\mathrm{e}^{\mathrm{i}sL}\, \Lambda^{(L)}(-s)}{(k_0+s)^2\,(s-k)\,K_-(s)}\,\mathrm{d}s \tag{3.11}$$

and two similar equations obtained by interchanging 0 and L in (3.10) and (3.11). These equations are to be completed via conditions (2.30) which we reproduce for completeness. Thus

$$\Lambda^{(*)}(k) = Q^{(*)}(k) \tag{3.12}$$

at all roots of $P(k) = 0$. Note that (3.9) and (3.12) provide the solution of the semi-infinite problem if we set $\hat{a}_n^{(*)}$ and $\Omega_-^{(*)}$ to zero.

The formal solution (3.9)–(3.12) contains all elements of the problem and can be thought of as a set of integral equations for the unknown functions $\Lambda^{(*)}(k)$. This was the formulation referred to in the introduction. From (3.9) it appears that $\Lambda^{(*)}$ contains the unknown constants $\hat{a}_n^{(*)}$, $E_n^{(*)}$ and the unknown function $\Omega_-^{(*)}$. Corresponding to the $N+4$ unknown constants per edge ($\hat{a}_n^{(*)}$, $E_n^{(*)}$ and the two implicit in $Q^{(*)}$) we have $N+4$ equations (3.10) and (3.12). The integral equation (3.11) corresponds likewise with the unknown function $\Omega_-^{(*)}$. We describe a method for the reduction to an infinite set of simultaneous linear equations in §5, while we devote §4 to a discussion of the approximation which results if we simply set $\Omega_-^{(*)} = 0$ in (3.9) and ignore equation (3.11). This approximation yields the same results as the informal approach of taking two semi-infinite edges and allowing them to communicate via the free-modes of propagation on an infinite plate. Such an informal approximation procedure has been used by Abrahams (1981) and Crighton & Innes (1984) for strip problems in the low frequency, heavy-fluid-loading limit. It

PHILOSOPHICAL TRANSACTIONS OF THE ROYAL SOCIETY A MATHEMATICAL, PHYSICAL & ENGINEERING SCIENCES

also forms an intrinsic part of the ray theory for cracks in elastic media, where the propagating mode in question is the Rayleigh wave (see, for example, Achenbach *et al.* 1982).

In the remainder of this paper we set the fluid dissipation to zero. This has the effect of causing the branch points at $k = \pm k_0$ to move onto the real axis. We can then obtain the far-field scattered pressure from (2.32) by using the method of steepest descent (see, for example, Noble 1958; Clemmow 1960). Thus

$$\psi \sim D(\theta_{\mathrm{rec}}, \theta_{\mathrm{inc}})\,(L/r)^{\frac{1}{2}}\,\mathrm{e}^{\mathrm{i}k_0 r}, \tag{3.13}$$

where D is the directivity function,

$$D = \{k_0/2\pi L\}^{\frac{1}{2}}\,\mathrm{e}^{-\mathrm{i}\pi/4}\sin\theta_{\mathrm{rec}}\,\tilde{\psi}(k_0\cos\theta_{\mathrm{rec}}), \tag{3.14}$$

and $x = -r\cos\theta_{\mathrm{rec}}$, $y = r\sin\theta_{\mathrm{rec}}$, θ_{rec} being the receiver angle.

4. The wide strip approximation

In this section we choose the branch cuts for γ to run vertically up from k_0 and down from $-k_0$. The contour C is chosen to run directly in contact with the cut which emanates from k_0: down the left-hand side and up the right-hand side of it.

Consider equation (3.11) which gives $\underset{\sim}{\Omega}^{(*)}$. The integrand contains the exponential factor $\mathrm{e}^{\mathrm{i}sL}$ which decays as $\mathrm{Im}\,(s)$ increases. This means that the important contributions to the integral come from the region $|s-k_0| = O(L^{-1})$ which decreases in size as L becomes large. Thus for sufficiently large L we suppose that we can neglect branch-cut contributions such as $\underset{\sim}{\Omega}^{(*)}$ in (3.9).

Using this approximation, we first provide an interpretation of the unknowns $\hat{a}_n^{(*)}$. Let us evaluate ψ on the strip $(0 < x < L,\ y = 0+)$ by using (2.31) and (2.32) as follows

$$\psi = \frac{1}{2\pi}\left\{\int_{-\infty}^{\infty}\frac{\Lambda^{(0)}(k)\,\mathrm{e}^{-\mathrm{i}kx}}{K(k)}\,\mathrm{d}k + \int_{-\infty}^{\infty}\frac{\Lambda^{(L)}(-k)\,\mathrm{e}^{\mathrm{i}k(L-x)}}{K(k)}\,\mathrm{d}k\right\}, \tag{4.1}$$

where we choose to indent the contours of integration to lie above $k = -k_{\mathrm{inc}}$ and $k = \hat{k}$ and below $k = -\hat{k}$; $\hat{k} > k_0$ being the real root of $K = 0$. In fact, since $\tilde{\psi}(k)$ has no poles, such choices are arbitrary, but necessary when we split the integral as in equation (4.1).

We deform the first integral in (4.1) to run around the branch-cut for γ in D_-. In the process, residue contributions are picked up from poles at $k = -k_{\mathrm{inc}}$ and $k = -\hat{k}_n$. Likewise, the second integral yields a branch-cut contribution from D_+ and residue contributions from $k = \hat{k}_n$. As before, we argue that we can ignore the branch-cut contributions when both x and $L-x$ are sufficiently large. The residue contributions yield

$$\psi \approx \sum_{n=1}^{N}\frac{\mathrm{i}}{K_+(\hat{k}_n)}\{b_n^{(0)}\,\mathrm{e}^{\mathrm{i}\hat{k}_n x} + \hat{b}_n^{(L)}\,\mathrm{e}^{\mathrm{i}\hat{k}_n(L-x)}\} - \frac{P(k_{\mathrm{inc}})\,\gamma_{\mathrm{inc}}}{K(k_{\mathrm{inc}})}\,\mathrm{e}^{\mathrm{i}k_{\mathrm{inc}}x}, \tag{4.2}$$

where

$$\hat{b}_n^{(*)} = \Lambda^{(*)}(-\hat{k}_n)/K'_-(\hat{k}_n). \tag{4.3}$$

Equation (4.2) may be easily interpreted. There are free modes of propagation of an infinite plate whose wavenumbers are $\hat{k}_n$. There is also a forced response given by the last term in (4.2) which is simply specular reflection from an infinite plate. The amplitude of the nth free mode coming out from the edge at $x = *$ is $\hat{b}_n^{(*)}$. Note

however that many of the free-mode wavenumbers have a significant imaginary part and the resulting exponential decay may make the mode in question small for the large values of x and $L-x$ at which we can neglect branch-cut contributions to obtain (4.2).

From (3.10) and (4.3) we have

$$\hat{a}_n^{(0)} = \mathrm{e}^{\mathrm{i}\hat{k}_n L}\hat{b}_n^{(L)},\ \hat{a}_n^{(L)} = \mathrm{e}^{\mathrm{i}\hat{k}_n L}\hat{b}_n^{(0)}, \tag{4.4}$$

which allows us to interpret $\hat{a}_n^{(*)}$ as the amplitude of free mode n incident on the edge at $x = *$ having originated at the other end of the strip.

Given the above interpretation in terms of free modes being exchanged between the edges it is natural to consider the edges in isolation. We have

$$\Lambda^{(*)} \approx K_-(k)\left\{E_0^{(*)} + E_1^{(*)}(k_0 - k) - \frac{b^{(*)}}{k + k_{\mathrm{inc}}^{(*)}} + \sum_{n=1}^{N}\frac{\hat{a}_n^{(*)}}{\hat{k}_n - k}\right\}, \tag{4.5}$$

when we neglect $\Omega_-^{(*)}$ in (3.9). Equation (3.12) yields a set of four equations allowing us to solve for $E_0^{(*)}$, $E_1^{(*)}$ and the two unknowns implicit in $Q^{(*)}$. The unknown incident wave amplitudes $\hat{a}_n^{(*)}$ are then considered as specified as far as this single edge is concerned. Equation (4.5) is of course precisely the one obtained from a semi-infinite analysis. Let us therefore suppose that we have used (3.12) to eliminate the unknowns $E_0^{(*)}$ and $E_1^{(*)}$ from (4.5). Thus

$$\Lambda^{(*)} \approx b^{(*)}\Lambda(k, \theta_{\mathrm{inc}}^{(*)}) + \sum_{n=1}^{N}\hat{a}_n^{(*)}\hat{\Lambda}_n(k), \tag{4.6}$$

where both $\Lambda(k,\theta)$ and $\hat{\Lambda}_n(k)$ are known functions.

We may now obtain the outgoing wave amplitudes $\hat{b}_n^{(*)}$ from (4.3) as

$$\hat{b}_n^{(*)} = b^{(*)}\hat{b}_n(\theta_{\mathrm{inc}}^{(*)}) + \sum_{m=1}^{N} R_{nm}\hat{a}_m^{(*)}, \tag{4.7}$$

where

$$\hat{b}_n(\theta) = \Lambda(-\hat{k}_n, \theta)/K'_-(\hat{k}_n) \tag{4.8}$$

and

$$R_{nm} = \hat{\Lambda}_m(-\hat{k}_n)/K'_-(\hat{k}_n). \tag{4.9}$$

The terms on the right-hand side of (4.7) can be interpreted as follows: the first represents the outgoing wave amplitude generated by an incident acoustic wave alone and the second represents the reflection of the incident free modes via a reflection matrix R_{nm}. The above results are precisely what one would obtain from the informal semi-infinite plate theory. When the propagation characteristics, (4.4), of the middle part of the strip are included, the resulting transmission–reflection problem can be solved by matrix inversion. Specifically, let Π be the propagation matrix, i.e.

$$\Pi_{\mathrm{nm}} = \delta_{\mathrm{nm}}\,\mathrm{e}^{\mathrm{i}\hat{k}_n L}; \tag{4.10}$$

and also let $\hat{\boldsymbol{a}}^{(*)}$ be a vector of the $\hat{a}_n^{(*)}$ and $\hat{\boldsymbol{b}}$ be a vector of the $\hat{b}_n$. We then find that, for instance,

$$\hat{\boldsymbol{a}}^{(0)} = (I - (\Pi R)^2)^{-1}\Pi\{b^{(L)}\hat{\boldsymbol{b}}(\theta_{\mathrm{inc}}^{(L)}) + b^{(0)}R\Pi\hat{\boldsymbol{b}}(\theta_{\mathrm{inc}}^{(0)})\}, \tag{4.11}$$

where the matrix inverse represents the infinity of multiple reflections across the strip. We emphasize once again that many of the free modes may be too rapidly decaying to make their way across from one edge to another; such modes simply produce negligible contributions.

Having determined the $\hat{a}_n^{(*)}$, we may obtain $A^{(*)}$ from (4.6), $\tilde{\psi}(k)$ from (2.31) and ψ from (2.32). The far-field can then be calculated via (3.3) if required.

As was mentioned before, the results of this section, which are obtained by the formal device of neglecting the term $\Omega_-^{(*)}$ in equation (3.9) for $A^{(*)}$ are the same as those obtained from informal, coupled semi-infinite plate theory. The object of the present study is to develop a method which may be used when this approximation is no longer valid, perhaps because the strip is not wide or because a pole of the integrand of (3.11) lies near to $k = k_0$, leading to a large value of the integrand there.

As an initial step towards this object, let us see how we might improve the approximation of this section. As was discussed earlier on, it is expected that the contributions to the integral for $\Omega_-^{(*)}$ in (3.11) should be predominantly from the region $|s-k_0| = O(L^{-1})$, for large values of L. Provided that $|k-k_0|L$ is large, we may then suppose that the factor $(s-k)$ in equation (3.11) may be approximated by k_0-k. This means that

$$\Omega_-^{(*)} \approx \text{const.} \times (k_0+k)^2/(k_0-k),$$

except near to $k = k_0$. An improved approximation can be based on this observation, but we are more concerned with cases for which L is not all that large. In the next section, we adopt a power series expansion for $\Omega_-^{(*)}$, of which the first term has the above form. The resulting formulation is then exact.

5. Reduction to simultaneous equations

We now describe the process whereby the integral equations of §3 are reduced to an infinite set of simultaneous equations. Our first observation is that $\Omega_-^{(*)}$ as given by (3.11) is analytic in the left half-plane $\mathrm{Re}\,(k) < 0$. This half-plane may in turn be mapped into the unit circle by the transformation $k \to (k_0+k)/(k_0-k)$, which suggests a power series in the variable $(k_0+k)/(k_0-k)$. In fact $\Omega_-^{(*)}/(k_0+k)$ is expanded in such a series.

We note that

$$\frac{1}{s-k} = 2k_0 \sum_{n=0}^{\infty} \frac{(k_0-s)^n\,(k_0+k)^n}{(k_0+s)^{n+1}\,(k_0-k)^{n+1}} \tag{5.1}$$

for $\mathrm{Re}\,(s) > 0$ and $\mathrm{Re}\,(k) < 0$. We suppose here and henceforth that the contour C lies in the right half-plane, $\mathrm{Re}\,(s) > 0$, so that (5.1) can be used in (3.11) to give

$$\Omega_-^{(*)}(k) = \frac{k_0+k}{k_0} \sum_{n=0}^{\infty} \bar{a}_n^{(*)} \left(\frac{k_0+k}{k_0-k}\right)^{n+1} \tag{5.2}$$

as the power series expansion of $\Omega_-^{(*)}$ where

$$\bar{a}_n^{(0)} = \frac{k_0^2}{\pi \mathrm{i}} \int_C \frac{A^{(L)}(-s)\,\mathrm{e}^{\mathrm{i}sL}(k_0-s)^n}{(k_0+s)^{n+3}K_-(s)}\,\mathrm{d}s \tag{5.3}$$

and $\bar{a}_n^{(L)}$ is given by the same equation with the symbols O and L interchanged.

The power series expansion is convergent in the domain $\mathrm{Re}\,(k) < 0$ so that (5.2) can be used in (3.9) to obtain $A^{(*)}$ there. Thus we find that

$$A^{(*)} = K_-(k)\left\{E_0^{(*)} + E_1^{(*)}(k_0-k) - \frac{b^{(*)}}{k+k_{\mathrm{inc}}^{(*)}} + \sum_{n=1}^{N} \frac{\hat{a}_n^{(*)}}{\hat{k}_n - k} + \frac{k_0+k}{k_0} \sum_{n=0}^{\infty} \bar{a}_n^{(*)} \left(\frac{k_0+k}{k_0-k}\right)^{n+1}\right\} \tag{5.4}$$

for $\mathrm{Re}\,(k) < 0$.

Now although (5.4) holds only in $\mathrm{Re}\,(k) < 0$ it may, for instance, be used in (5.3) to obtain

$$\bar{a}_n^{(0)} + \sum_{m=0}^{\infty} \bar{M}_{n+m}\, \bar{a}_n^{(L)} + \sum_{m=0}^{1} M_{nm}\, E_m^{(L)} + \sum_{m=1}^{N} \hat{M}_{nm}\, \hat{a}_m^{(L)} = b^{(L)} m_n(\theta_{\mathrm{inc}}^{(L)}), \tag{5.5}$$

where

$$\bar{M}_n = \frac{\mathrm{i}k_0}{\pi} \int_C \frac{K_-(-s)\, \mathrm{e}^{\mathrm{i}sL} (k_0 - s)^{n+2}}{K_-(s)\, (k_0 + s)^{n+4}}\, \mathrm{d}s, \tag{5.6}$$

$$M_{nm} = \frac{\mathrm{i}k_0^2}{\pi} \int_C \frac{K_-(-s)\, \mathrm{e}^{\mathrm{i}sL} (k_0 - s)^{n}}{K_-(s)\, (k_0 + s)^{3+n-m}}\, \mathrm{d}s, \tag{5.7}$$

$$\hat{M}_{nm} = \frac{\mathrm{i}k_0^2}{\pi} \int_C \frac{K_-(-s)\, \mathrm{e}^{\mathrm{i}sL} (k_0 - s)^{n}}{K_-(s)\, (k_0 + s)^{n+3}\, (\hat{k}_m + s)}\, \mathrm{d}s \tag{5.8}$$

and

$$m_n(\theta) = \frac{\mathrm{i}k_0^2}{\pi} \int_C \frac{K_-(-s)\, \mathrm{e}^{\mathrm{i}sL} (k_0 - s)^{n}}{K_-(s)\, (k_0 + s)^{n+3}\, (k_0 \cos\theta - s)}\, \mathrm{d}s. \tag{5.9}$$

equations (5.5) also holds with the symbols O and L interchanged. It provides an infinite set of simultaneous equations corresponding to the infinity of unknown coefficients $\bar{a}_n^{(*)}$ which we have now introduced.

When we use (5.4) in (3.1) to obtain an expression for $\Omega_-^{(*)}$ and then substitute into (3.9) we find that

$$\begin{aligned} \Lambda^{(0)} = K_-(k) \Bigg\{ & \sum_{n=0}^{1} E_n^{(0)} (k_0 - k)^n + \sum_{n=1}^{N} \frac{\hat{a}_n^{(0)}}{\hat{k}_n - k} - \frac{b^{(0)}}{k + k_{\mathrm{inc}}^{(0)}} \\ & + \sum_{n=0}^{\infty} \bar{a}_n^{(L)}\, \bar{\Omega}_n(k) + \sum_{n=0}^{1} E_n^{(L)}\, \Omega_n(k) + \sum_{n=1}^{N} \hat{a}_n^{(L)}\, \hat{\Omega}_n(k) + b^{(L)} \Omega(k, \theta_{\mathrm{inc}}^{(L)}) \Bigg\}, \end{aligned} \tag{5.10}$$

where

$$\bar{\Omega}_n(k) = \frac{(k_0 + k)^2}{2\pi \mathrm{i} k_0} \int_C \frac{K_-(-s)\, \mathrm{e}^{\mathrm{i}sL} (k_0 - s)^{n+2}}{K_-(s)\, (k_0 + s)^{n+3}\, (s - k)}\, \mathrm{d}s, \tag{5.11}$$

$$\Omega_n(k) = \frac{(k_0 + k)^2}{2\pi \mathrm{i}} \int_C \frac{K_-(-s)\, \mathrm{e}^{\mathrm{i}sL} (k_0 + s)^{n-2}}{K_-(s)\, (s - k)}\, \mathrm{d}s, \tag{5.12}$$

$$\hat{\Omega}_n(k) = \frac{(k_0 + k)^2}{2\pi \mathrm{i}} \int_C \frac{K_-(-s)\, \mathrm{e}^{\mathrm{i}sL}}{K_-(s)\, (s - k)\, (k_0 + s)^2\, (\hat{k}_n + s)}\, \mathrm{d}s \tag{5.13}$$

and

$$\Omega(k, \theta) = \frac{(k_0 + k)^2}{2\pi \mathrm{i}} \int_C \frac{K_-(-s)\, \mathrm{e}^{\mathrm{i}sL}}{K_-(s)\, (s - k)\, (k_0 + s)^2\, (s - k_0 \cos\theta)}\, \mathrm{d}s. \tag{5.14}$$

Equation (5.10) also gives $\Lambda^{(L)}$ when O and L are interchanged. These expressions are valid for all k and give $\Lambda^{(*)}$ in terms of the unknowns $E_n^{(*)}$, $\hat{a}_n^{(*)}$ and $\bar{a}_n^{(*)}$.

We now have the complete set of simultaneous equations to solve. These consists of (3.10) and (3.12) (using expression (5.10) for $\Lambda^{(*)}$) together with (5.5). The former two correspond to the unknowns $\hat{a}_n^{(*)}$ and $E_n^{(*)}$ (and those implicit in $Q^{(*)}$), while the latter correspond to the unknowns $\bar{a}_n^{(*)}$ which we have introduced in this section. Once this set of equations has been solved, $\tilde{\psi}$ can be obtained from (2.31) and (5.10). Thus we have succeeded in our object of reducing the scattering problem to a set of simultaneous equations. It will, however, be appreciated that there remain the

computational problems of actually calculating the various contour integrals and solving the equations. These issues are addressed in Appendixes A, B and C.

6. Discussion

We have presented an analysis of the scattering by a finite elastic strip which leads to an infinite set of simultaneous equations in an infinite number of unknowns. This represents an extension of the Wiener–Hopf technique from the coupled pair of integral equations which result when it is applied to finite problems.

The numerical implementation of the method involves the truncation of the infinite set of equations. An outline proof that this truncation procedure approaches the solution of the infinite problem as the number of unknowns increases is given in Appendix D.

Numerical solution of the equations derived in this paper requires the computation of certain contour integrals. Firstly, the multiplicative split of the kernel requires such evaluations and is described in Appendix B. The remaining contour integrals were introduced in §5 and their evaluation is described in Appendix C. The main concern is to ensure that any singularities of the integrand are either kept away from the integration contour or are removed prior to numerical evaluation. The methods used probably have fairly wide applications; similar methods have been used by the author to evaluate the numerical splits of Wiener–Hopf kernels of a number of different problems.

Some results obtained from the calculations are shown in figure 3. They show plots of far-field scattered pressure where the receiver and source share the same value of θ. The strip has free edges and an aspect ratio $L/h = 20$, h being the plate thickness. The fluid and strip have the properties of water and steel respectively. The plot in figure 3*a* is for a frequency of 0.428 times the coincidence frequency for the plate. Figure 3*b*–*d* shows plots for increasing frequencies up to 2.14 times the coincidence frequency in figure 3*d*. A specular reflection of decreasing angular width and increasing number of side-lobes is evident in all plots. This is to be expected of course. Figure 3*b* and *c* (at 0.856 and 1.07 times the coincidence frequency) shows the emergence of another distinct feature which persists to higher frequencies and can clearly be identified as being due to the 'leaky' wave (see Crighton 1979).

The above cases were also treated using the approximation of §4, which we have shown to be equivalent to taking two semi-infinite plates and allowing them to communicate through the modes of an infinite plate. The results are not shown here, but are very similar to those obtained via the exact method. Differences of the order of 10% in intensity (or about 0.5 dB) were typical but varied significantly with frequency and angle. Thus a rough idea of the scattering strength can be obtained from the approximate method, but more accurate results require the full analysis. We should also mention that other cases we have tried, involving acoustic scattering from finite elastic cylinders, can produce gross discrepancies in some ranges of frequency and angle. This occurred when there was a mode of propagation on the infinite cylinder whose wavenumber was close to the acoustic wavenumber, k_0.

Figures 4 and 5 show results as a function of frequency for two angles ($\theta = 72°$ and 36°). Resonances of the plate are evident below the coincidence frequency. The resonant contributions have decreasing strength and increasing width as frequency increases towards coincidence. For the purposes of comparison, these figures show the corresponding results if the plate were infinitely stiff as a dashed line.

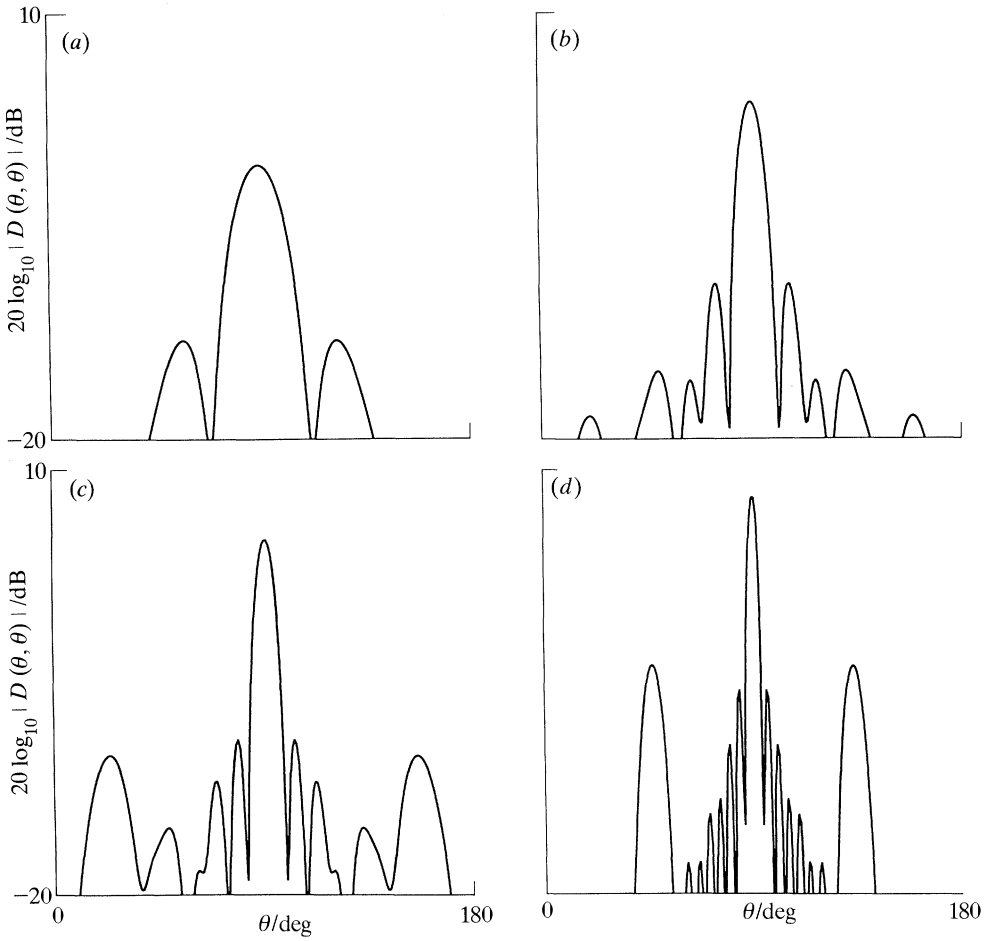

Figure 3. Plot of $20 \log_{10} |D(\theta, \theta)|$ against θ for the following multiples of the coincidence frequency: (*a*) 0.428, (*b*) 0.856, (*c*) 1.07 and (*d*) 2.14.

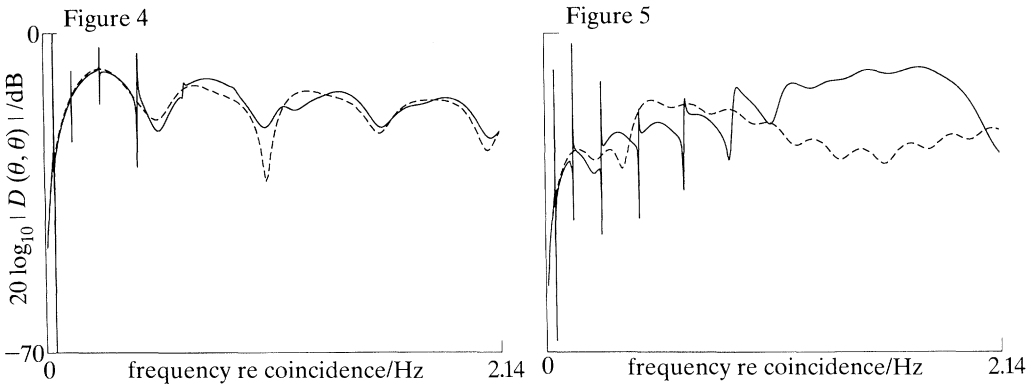

Figure 4. $20 \log_{10} |D(\theta, \theta)|$ against frequency for $\theta = 72°$; the dashed line shows the result for a rigid strip.

Figure 5. $20 \log_{10} |D(\theta, \theta)|$ against frequency for $\theta = 36°$; the dashed line shows the result for a rigid strip.

The problem analysed in this paper had the incident plane wavefront parallel to the edge of the strip. Oblique incidence (i.e. with sinusoidal variation along the edge of the strip) can be treated by the same techniques, involving only a slightly more complicated formulation. I have not included this here because I wish to present the methods as clearly as possible.

The methods described here are applicable to many finite problems. I intend to present further work on such problems shortly.

Appendix A. Numerical implementation

From an analytical point of view the choice of branch cut for γ is largely arbitrary. However, numerically we wish to avoid poles of the integrand which lie near to the contours of integration. In particular it will turn out that the integrals in equations (5.6)–(5.9) and (5.11)–(5.14), whose evaluation is described in Appendix C lead to pole singularities at the roots of $\gamma^2 P^2 = 1$. We choose the branch cuts for γ to lie along straight lines given by

$$k = \pm (k_0 + u\zeta), \tag{A 1}$$

where u is a positive real parameter and $\zeta = \mathrm{e}^{\mathrm{i}\phi}$ with $\frac{1}{4}\pi < \phi < \frac{1}{2}\pi$.

The angle ϕ that the cuts make with the real axis is chosen as follows. Each of the roots of the polynomial equation $\gamma^2 P^2 = 1$ is examined. The value of $\arg(k - k_0)$ gives the angle of the root, k, as seen from k_0. For any given value of ϕ we can calculate the angular 'distance' of the cut to each root and to $\phi = \frac{1}{4}\pi, \frac{1}{2}\pi$. The 'nearest' of these possibilities, i.e. the above roots or $\phi = \frac{1}{4}\pi, \frac{1}{2}\pi$, gives a measure of the proximity of the cut to the closest problem area. This angular distance is maximized, yielding a value for ϕ as far as possible from any problems.

The above choice of cuts is of course only one of many possible prescriptions; it is satisfactory because it keeps the cuts away from the roots of $\gamma^2 P^2 = 1$, which was our objective. The value of γ can then be determined from

$$\gamma = -\mathrm{i}\zeta((k_0 - k)/\zeta)^{\frac{1}{2}}((k_0 + k)/\zeta)^{\frac{1}{2}}, \tag{A 2}$$

where the square roots are principal values.

The next problem is to determine the roots of $K(k) = 0$. Looked at as a function of γ, $K = 1 - \gamma P$, is a quintic polynomial with real coefficients for which the roots can be found by a standard polynomial solver. The difficulty is to refer these roots back to roots of $K(k) = 0$ in the complex k-plane. There will always be a positive real γ-root which can be directly related to $\hat{k} = (\gamma^2 + k_0^2)^{\frac{1}{2}}$. This root is identified and used to calculate $\hat{k}_N$. The other γ-roots are dealt with as follows. For each γ-root define a value of k by

$$k = \pm (\gamma^2 + k_0^2)^{\frac{1}{2}}, \tag{A 3}$$

with the sign chosen so that either k is real and positive or $\mathrm{Im}(k) > 0$. This value of k may or may not be a root of $K = 0$ (but it will be a root of $\gamma^2 P^2 = 1$). If k lies to the left of the branch cut emanating from $k = k_0$ and the original γ-root is in $\mathrm{Im}(\gamma) < 0$ then k is one of the $\hat{k}_n$. Roots which give a value of k to the right of the branch cut and for which $\mathrm{Im}(\gamma) > 0$, $\mathrm{Re}(\gamma) > 0$ are also to be included in the $\hat{k}_n$. Thus $\hat{k}_1, \ldots, \hat{k}_{N-1}$ are determined.

The contour C used in the integrals of (5.6)–(5.9) and (5.11)–(5.14) was specified by the requirement that all pole singularities of the integrands should lie outside of C.

One such singularity is the real root, $\hat{k}$, which has the property that it may approach the point $k = k_0$ closely at frequencies above the coincidence frequency for the plate. In this case, the numerical conditioning of the proposed method can become poor and it is appropriate to include the corresponding pole singularity in $\Omega_-^{(*)}$ when writing $H_-^{(*)}$ in the form (3.2). This has the effect of (i) excluding $\hat{k}$ from the set of roots of $K = 0$ (thus reducing N by one) and (ii) redefining C to include the pole at the real root. The method is otherwise unchanged.

Having determined the set of roots, $\hat{k}_n$, the next problem is to calculate $K_+(k)$ and each of the quantities defined by equation (5.6)–(5.9) and (5.11)–(5.14). The numerical procedures adopted are described in Appendixes B and C. This allows us to determine the coefficients of the infinite set of linear simultaneous equations for the unknowns with their right-hand sides (one for each angle of incidence). For numerical purposes we truncate the set of unknowns $\bar{a}_n^{(*)}$ to a finite number and correspondingly make the number of equations of the form (5.5) finite. The demonstration that the truncated solutions approach the true solution as the number of unknowns increases is given in Appendix D. A standard matrix equation solver then determines the unknowns of the problem for each angle of incidence. At this stage $\Lambda^{(*)}$ can be calculated for any value of complex k by using equation (5.10). The quantity $\tilde{\psi}$ can be obtained from (2.31) and ψ from (2.32) if required. In fact, we are interested in the far-field, which is given by equation (3.13).

In calculating the far-field, the reader should note the problem that, if we set $\theta_{\mathrm{rec}} = \pi \pm \theta_{\mathrm{inc}}$, both $\Lambda^{(0)}(k_0 \cos\theta_{\mathrm{rec}})$ and $\Lambda^{(L)}(-k_0 \cos\theta_{\mathrm{rec}})$ are infinite due to their pole at $k = -k_{\mathrm{inc}}^{(*)}$. These poles should cancel each other out when ψ is formed from equation (2.31) and this limit must first be taken analytically. We do not give the details here, but it involves calculating $K_+'(k)/K_+(k)$, which is the additive Cauchy split of $K'(k)/K(k)$ and can be computed via a method similar to that described for Y_+ in Appendix B. We also note that cases where θ_{rec} or θ_{inc} are zero or π lead to zero scattered field and, as such, do not need to be computed.

Apart from making the usual checks on numerical convergence (namely observing the effect of increasing the number of integration points in all integrals and the number of truncated $\bar{a}_n^{(*)}$) we also verified that reciprocity and energy conservation conditions were satisfied. The former leads to $D(\theta, \theta') = D(\theta', \theta)$ (D being the directivity function defined in §3) while the latter can be expressed via the identity

$$\int_0^{\pi} |D|^2(\theta, \theta')\, \mathrm{d}\theta' = \left(\frac{2\pi}{k_0 L}\right)^{\frac{1}{2}} \mathrm{Re}\,(\mathrm{e}^{\mathrm{i}\pi/4} D(\pi - \theta, \theta)). \tag{A 4}$$

Appendix B. The numerical split of the kernel

Let

$$Y(k) = \ln\left\{-2\rho_0 \omega^2 K(k)\, \gamma^{2N-5}/B \prod_{n=1}^{N} (k^2 - \hat{k}_n^2)\right\} \tag{B 1}$$

so that $Y(k)$ is analytic apart from the branch cuts for γ and the branch of ln is chosen so that $Y(k) \to 0$ as $k \to \infty$.

We perform a Cauchy integral split of $Y(k)$, i.e.

$$Y_+(k) = \frac{1}{2\pi \mathrm{i}} \int_{C_1} \frac{Y(s)}{s - k}\, \mathrm{d}s, \tag{B 2}$$

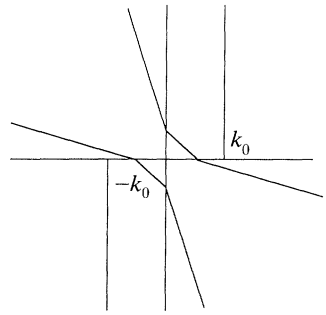

Figure 6. The complex k-plane showing the 'tunnel' within which the pole is removed from the integrand.

where the contour C_1 lies in the strip D, runs from $s = -\infty$ to $s = +\infty$ and lies below $s = k$.

The contour of integration is next deformed onto the diagonal line, $s = (1-\mathrm{i})\,tk_0$, where t is a real parameter. Since $Y(k) = Y(-k)$ we can write

$$Y_+(k) = Y_1 - \frac{k_0\,k(1+\mathrm{i})}{\pi}\int_0^\infty \frac{Y(s)}{s^2-k^2}\,\mathrm{d}t, \tag{B 3}$$

where Y_1 is the residue contribution occurring from the contour deformation if it crosses the pole at $s = k$, i.e.

$$Y_1 = Y(k), \tag{B 4}$$

if $\mathrm{Re}\,(k) < -\mathrm{Im}\,(k)$ and $Y_1 = 0$ otherwise.

For values of k near the diagonal contour we wish to remove the pole singularity from the integral to improve numerical conditioning. In this case we have

$$Y_+(k) = Y_1 + Y_2 - \frac{k_0\,k(1+\mathrm{i})}{\pi}\int_0^\infty \frac{Y(s)-Y_0}{s^2-k^2}\,\mathrm{d}t, \tag{B 5}$$

where $Y_2 = \frac{1}{2}Y_0$ if $\mathrm{Re}\,(k) > -\mathrm{Im}\,(k)$ and $Y_2 = -\frac{1}{2}Y_0$ if $\mathrm{Re}\,(k) < -\mathrm{Im}\,(k)$. Equation (B 5) is obtained from (B 3) by using an identity valid for any value of Y_0; in practice we set $Y_0 = Y(k)$ when we wish to eliminate the pole and $Y_0 = 0$ otherwise.

To be specific about when we remove the pole, we define a 'tunnel' in the complex k-plane as shown in figure 6. Points lie within the tunnel when

$$|\mathrm{Im}\,(k) + \mathrm{Re}\,(k)| < \tfrac{1}{2}\max\left(|\mathrm{Im}\,(k) - \mathrm{Re}\,(k)| - \tfrac{1}{2}k_0,\, k_0\right) \tag{B 6}$$

and for such values of k we remove the pole by setting $Y_0 = Y(k)$. The above choice of region is of course somewhat arbitrary.

We may transform the infinite integration range in (B 5) into a finite range by setting $u = 1/(1+t)$. Thus we have

$$Y_+(k) = Y_1 + Y_2 - \frac{k_0\,k(1+\mathrm{i})}{\pi}\int_0^1 \frac{Y(s)-Y_0}{(s^2-k^2)\,u^2}\,\mathrm{d}u, \tag{B 7}$$

where

$$s = (1-\mathrm{i})\,k_0(1-u)/u \tag{B 8}$$

and according to the above prescription:

(i) above the tunnel we set $Y_0 = Y_1 + Y_2 = 0$;

(ii) within the tunnel $Y_0 = Y(k)$ and $Y_1 + Y_2 = \frac{1}{2}Y(k)$;

(iii) below the tunnel we have $Y_0 = 0$ and $Y_1 + Y_2 = Y(k)$.

Once $Y_+(k)$ is known, the product split of the kernel can be obtained from

$$K_+(k) = \mathrm{i}\,\mathrm{e}^{Y_+}\left(\frac{B}{2\rho_0\omega^2}\right)^{\frac{1}{2}}\left[(-\mathrm{i}\zeta)^{\frac{1}{2}}\left(\frac{k+k_0}{\zeta}\right)^{\frac{1}{2}}\right]^{5-2N}\prod_{n=1}^{N}-\mathrm{i}(k+\hat{k}_n), \tag{B 9}$$

with ζ defined as in Appendix A. The somewhat obscure way of writing the term in square brackets places the branch cut for K_+ in the same place as the cut for γ when principal values are used for the complex square roots.

The integral in (B 7), being that of a smooth function, can be evaluated by any standard numerical integration rule. From the point of view of efficiency, a set of fixed integration points at which $Y(s)$ is needed is an advantage because these do not then have to be recalculated every time that $Y_+(k)$ is required for a new value of k. This is particularly important since $K_+(k)$ is required at a large number of points.

The calculation of $Y(s)$ from equation (B 1) involves the computation of a complex logarithm. This logarithm is defined to be zero at $s = \infty$, but its value at other points is initially undetermined to within a multiple of $2\pi\mathrm{i}$. Continuity along the integration contour is invoked. Thus the value of $Y(s)$ is computed at integration points starting from $s = \infty$, i.e. $u = 0$, stepping towards smaller values of s. Where the argument of ln crosses the branch cut for the particular implementation of the ln function this fact is noted and the appropriate multiple of $2\pi\mathrm{i}$ is determined so that $Y(s)$ is continuous.

The multiple valued nature of the complex logarithm is also of concern if $Y(k)$ is needed. In fact, changing the value of $Y(k)$ which is used to compute both Y_0 and $Y_1 + Y_2$ by a multiple of $2\pi\mathrm{i}$ will not change the calculated value of $K_+(k)$. However, it will be recalled that within the tunnel the object is to remove the pole singularity to improve numerical conditioning. For this reason the correct branch of ln is needed when the pole lies near the contour.

The procedure adopted in choosing $Y(k)$ when k lies within the tunnel is as follows: (i) find the integration point nearest k (i.e. with the smallest value of $|s-k|$); (ii) since the value of $Y(s)$ is known at this point, find the appropriate multiple of $2\pi\mathrm{i}$ which places $Y(k)$ as close to $Y(s)$ as possible.

The computational work was organized as follows. Two routines were written: one set up a number of quantities including arrays of values for s and $Y(s)$ at the integration points. A second routine was called whenever a value of $K_+(k)$ was required: this routine determined where k lies relative to the tunnel, calculated Y_0 and $Y_1 + Y_2$, performed the numerical integral and determined K_+ from (B 9). The accuracy of the results were determined by varying the number of integration points.

We note that

$$K_-(k) = K_+(-k) \tag{B 10}$$

may be used to evaluate K_- when required, while

$$K'_-(\hat{k}_n) = K'(\hat{k}_n)/K_+(\hat{k}_n) \tag{b 11}$$

provides a straightforward way of formulating the set of equations (3.10).

Appendix C. The contour integrals

The contour integrals in (5.6)–(5.9) and (5.11)–(5.14) are each of the form

$$I = \int_C \frac{K_-(-s)\,\mathrm{e}^{\mathrm{i}sL}}{K_-(s)} f(s)\,\mathrm{d}s \tag{C 1}$$

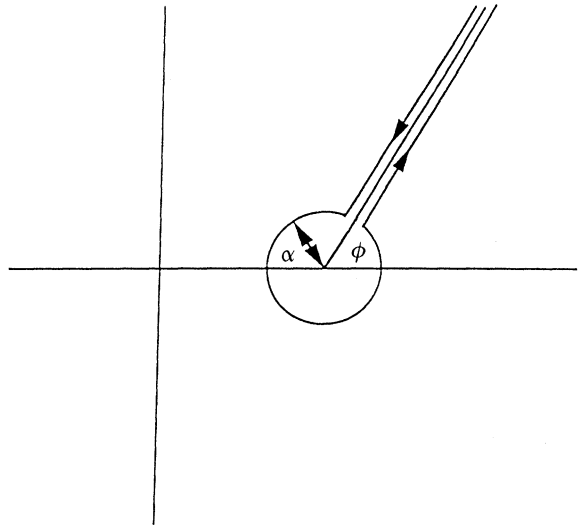

Figure 7. The complex k-plane showing the contour of integration used for numerical computation.

with a variety of expressions for $f(s)$, none of which exhibit branch cuts. Since $K_-(-s) = K_+(s)$ and $K(s) = K_+(s)\,K_-(s)$ we can rewrite (C 1) as

$$I = \int_C \frac{K_+^2(s)\,\mathrm{e}^{\mathrm{i}sL}}{K(s)} f(s)\,\mathrm{d}s, \tag{C 2}$$

or

$$I = \int_C \frac{F(s)}{K(s)}\,\mathrm{d}s, \tag{C 3}$$

where $F(s) = K_+^2(s)\,\mathrm{e}^{\mathrm{i}sL} f(s)$ has no branch cut in the region of interest, $\mathrm{Re}\,(s) > 0$.

The contour, C, was originally required to exclude all poles of the integrand, with the possible exception of the real root of $K = 0$, as described in Appendix A. In fact, the contour we use for numerical integration is as shown in figure 7 and consists of a section running down the left side of the cut, around a circle of radius α centred at $s = k_0$ and up the right side of the cut. The radius α was chosen as follows: let

$$\alpha_0 = \min\,(L^{-1}, \tfrac{1}{2}k_0, \tfrac{1}{3}|k_0 - \hat{k}_n|, \tfrac{1}{3}|k_0 + \hat{k}_n|), \tag{C 4}$$

where the minimum is to be taken over all $\hat{k}_n$ except the real root. There are then three cases:

(i) if $|\hat{k} - k_0| \geqslant 2\alpha_0$, we set $\alpha = \alpha_0$;

(ii) if $\alpha_0 \leqslant |\hat{k} - k_0| < 2\alpha_0$, we set $\alpha = \frac{1}{2}|\hat{k} - k_0|$;

(iii) if $|\hat{k} - k_0 < \alpha_0$, we set $\alpha = \alpha_0 + \frac{1}{2}|\hat{k} - k_0|$.

It is only in case (iii) that the real root lies inside C. In this case the root $\hat{k}$ is dropped from the set of roots, $\hat{k}_n$, for the purpose of calculating $A^{(*)}$ from (5.10) and the corresponding equation of the form (3.10) is also dropped.

The above choice of contour succeeds in keeping all the roots of $K = 0$ at a distance. However, in the calculation of $m_n(\theta)$ and all of the Ω(s) there are poles at $s = k_0 \cos\theta$ or $s = k$ which can lie inside the circle $|s - k_0| = \alpha$. These poles then violate the requirement that all poles should lie outside C. Even if they lie outside C, but are close to the contour, they can lead to numerical problems.

The above problems can be resolved by removal of the offending poles as follows. The poles in question lie at $s = \beta$ where $\beta = k$ or $\beta = k_0 \cos\theta$. When there are no such poles of the integrand with $|\beta - k_0| < \frac{3}{2}\alpha$ we ignore them and use (C 3) directly. This is always the case with the integrals of (5.6)–(5.8) for instance.

When there is just one pole with $|\beta - k_0| < \frac{3}{2}\alpha$ we may instead use

$$I = \int_C F(s)\left[\frac{1}{K(s)} - \frac{1}{K(\beta)}\right]\mathrm{d}s, \tag{C 5}$$

which removes the pole and corrects the value of I when β lies inside C. Two poles, β_1, β_2 which both lie in $|\beta - k_0| < \frac{3}{2}\alpha$ can be dealt with using

$$I = \int_C F(s)\left[\frac{1}{K(s)} - A_1 - A_2(2s - \beta_1 - \beta_2)\right]\mathrm{d}s, \tag{C 6}$$

where $$A_1 = \tfrac{1}{2}\left(\frac{1}{K(\beta_1)} + \frac{1}{K(\beta_2)}\right) \quad \text{and} \quad A_2 = \frac{1}{2(\beta_2 - \beta_1)}\left(\frac{1}{K(\beta_1)} - \frac{1}{K(\beta_2)}\right). \tag{C 7}$$

In the case when $\beta_1 = \beta_2$ the limit of (C 7) should be taken so that

$$A_2 = -K'(\beta)/2K^2(\beta). \tag{C 8}$$

The above results can be summarized as follows:

$$I = \int_C F(s)\, g(s)\, \mathrm{d}s, \tag{C 9}$$

where $$g(s) = 1/K(s), \tag{C 10}$$

if there is no offending pole,

$$g(s) = 1/K(s) - 1/K(\beta), \tag{C 11}$$

when there is one such pole, at $s = \beta$, and

$$g(s) = 1/K(s) - A_1 - A_2(2s - \beta_1 - \beta_2), \tag{C 12}$$

when there are two, at $s = \beta_1, \beta_2$.

We can write

$$s = k_0 + \alpha\zeta/(1 - t) \tag{C 13}$$

for the part of C which runs along the branch cut and

$$s = k_0 + \alpha\zeta\, \mathrm{e}^{\mathrm{i}2\pi v}. \tag{C 14}$$

for the circular part of C. Let $\vec{\gamma}$ denote the value of γ just to the right of the branch-cut. The value of K on the two sides is then $K = 1 - \vec{\gamma}P(s)$ to the right and $K = 1 + \vec{\gamma}P(s)$ to the left. Thus the integral contribution from the cut is

$$I_1 = 2\alpha\zeta \int_0^1 \frac{\vec{\gamma}P(s)\, F(s)}{(1-t)^2\,(1 - \gamma^2 P^2(s))}\,\mathrm{d}t, \tag{C 15}$$

where $\vec{\gamma}$ can be determined from $\vec{\gamma} = (s^2 - k_0^2)^{\frac{1}{2}}$ with a principal value for the square root. The integral contribution from the circle is given by

$$I_2 = 2\pi\mathrm{i} \int_0^1 F(s)\, g(s)\, (s - k_0)\, \mathrm{d}v. \tag{C 16}$$

The above integrals are computed using a standard integration rule. As was the case with evaluating the kernel split, fixed integration points can be exploited via an initialization routine which sets up arrays of values which are repeatedly used when evaluating different integrals. The number of integration points is, as always, varied to provide a check on accuracy.

Appendix D. Convergence of the truncated solutions

We regard the combination of $\hat{a}_n^{(0)}$, $E_n^{(0)}$, the two unknowns from the edge polynomial $Q^{(0)}$ and the infinite set, $\bar{a}_n^{(0)}$, as an infinite complex vector. A similar vector can be formed from the corresponding unknowns with 0 replaced by L. This pair of vectors can be taken as an element of Hilbert space with the usual norm and inner product. We give the outline of a proof that the truncated equations lead to solutions which converge to the solution of the infinite set of equations as the number increases to infinity.

The infinite set of equations, as specified in §5, can be written as

$$(I+A)\,a = b, \tag{D 1}$$

where a is the infinite solution vector, b is the vector of right-hand sides, A is a linear operator and I is the identity operator. The Fredholm theory of infinite-dimensional Banach spaces can be applied provided that

$$\sum_{m,\,n=0}^{\infty} |\bar{M}_{n+m}|^2 < \infty, \tag{D 2}$$

$$\sum_{n=0}^{\infty} |M_{nm}|^2 < \infty, \tag{D 3}$$

$$\sum_{n=0}^{\infty} |\bar{\Omega}_n(k)|^2 < \infty, \tag{D 4}$$

and

$$\sum_{n=0}^{\infty} |m_n(\theta)|^2 < \infty \tag{D 5}$$

hold. In this case (D 1) has a unique solution, provided there is no non-trivial solution of

$$(I+A)\,a = 0. \tag{D 6}$$

It can be shown, by tracing the arguments used in the paper backwards, that a non-trivial solution of (D 6) implies a non-trivial solution of the original diffraction problem with no incident wave. We disregard this possibility on physical grounds.

Truncation of the set of infinite equations leads to a sequence of operators A_n and right-hand sides b_n such that $b_n \to b$ and $A_n \to A$ (with the usual operator norm), provided that conditions (D 2)–(D 5) hold. The truncated solutions are $a_n = (I+A_n)^{-1} b_n$ and since $(I+A)$ is invertible $(I+A_n)^{-1} \to (I+A)^{-1}$. It then follows that $a_n \to (I+A)^{-1} b$, the solution of the infinite problem.

It remains to show that (D 2)–(D 5) hold. We demonstrate (D 2) noting that the proof of the others is similar.

The convergence of the series in (D 2) is determined by the behaviour of $|\bar{M}_n|$ as $n \to \infty$. Provided that $|\bar{M}_n|$ is sufficiently rapidly decreasing, the series will converge.

The definition of $\bar{M}_n$ is equation (5.6). The integrand depends on n through the factor.

$$((s-k_0)/(s+k_0))^n, \tag{D 7}$$

whose modulus can be written

$$\exp[-n\ln|(s+k_0)/(s-k_0)|] \tag{D 8}$$

and decays exponentially with n for any fixed value of complex s. However, for large values of $|s|$, the decay rate with n becomes small. This indicates that the behaviour of $\bar{M}_n$ for large n is dictated by large values of $|s|$ in the integral. As we shall see, it is the balance between the decrease of the factor (D 7) with increasing n and the decrease of e^{isL} with increasing $\mathrm{Im}(s)$ which determines the form of $\bar{M}_n$ as $n\to\infty$.

The product of the above two factors can be written as e^{ϕ}, where

$$\phi = isL + n\ln((s-k_0)/(s+k_0)) \tag{D 9}$$

and we use the method of steepest descent. The saddle point, where $d\phi/ds = 0$, occurs at

$$s_0 = k_0(1+2in/k_0L)^{\frac{1}{2}} \tag{D 10}$$

and the steepest descent path is given by $\mathrm{Im}(\phi) = \text{constant}$ and runs through s_0. For large enough n, the path can also be shown to go through $s = k_0$ and to asymptote to the line $\mathrm{Re}(s) = L^{-1}\,\mathrm{Im}(\phi(s_0)) > 0$ as $\mathrm{Im}(s)\to+\infty$.

For large values of n we may approximate ϕ by

$$\phi \sim (nk_0L)^{\frac{1}{2}}(i\sigma - 2\sigma^{-1}) \tag{D 11}$$

for σ of order one where $\sigma = (L/nk_0)^{\frac{1}{2}}s$. Under this approximation, the steepest descent path is given by

$$\sigma_2 = [1\pm(1-\sigma_1^2(2-\sigma_1)^2)^{\frac{1}{2}}]/(2-\sigma_1), \tag{D 12}$$

where $\sigma = \sigma_1 + i\sigma_2$. The + sign in (D 12) is taken for $0<\sigma_1<1$ and the minus sign when $1<\sigma_1<2$. The path specified by (D 12) starts at the origin tangential to the real σ-axis, passes smoothly through the saddle point $\sigma = 1+i$ and then asymptotes to $\sigma_1 = 2$, $\sigma_2 = +\infty$ (σ_2 is an increasing, positive function of σ_1, in $0<\sigma_1<2$). The above description does not, of course, describe the region where $|s| = O(k_0)$ as $n\to\infty$. In this region

$$s_2 = (L/nk_0)^{\frac{1}{2}}(s_1^2 - k_0^2), \tag{D 13}$$

where $s = s_1 + is_2$ and $s_1 > k_0$.

We wish to change the branch cut of γ emanating from $s = k_0$ so that it lies along the steepest descent path, at least for large $|s|$ of order $(nk_0/L)^{\frac{1}{2}}$. The contour of integration in (5.6) is also deformed to lie around, and in contact with, the new branch cut. For such a change in contour to leave the integral unaffected we require that no poles of the integrand appear or disappear due to the change in cut.

There are a finite number of possible poles that all lie in $|s|<S$, say. If we choose the branch cut for γ to coincide with the original one for $|s|<S$ and with the steepest descent path for $|s|>2S$ then there need be no changes in poles due to the change in branch cut.

It follows from the discussion following equation (D 7) that the integral along the contour in $|s|<2S$ can be bounded above by an exponential term of the form α^n with

$\alpha < 1$. The remaining part of the contour lies along the steepest descent path and as $s \to \infty$ the integrand has the asymptotic form

$$\pm (\mathrm{i}/s^2)\,(-1)^n\,\mathrm{e}^{\phi} \tag{D 14}$$

where the + sign applies to the left of the branch cut and the − sign should be used to the right of the cut. As $n \to \infty$, the exponential factor in (D 14) is dominant near the point $s = s_0$. The usual steepest descent argument involves the expansion of ϕ about $s = s_0$ thus

$$\phi = \phi(s_0) + (L^2/2n)\,(1 + 2\mathrm{i}n/k_0 L)^{\frac{1}{2}}(s - s_0)^2. \tag{D 15}$$

The integral has the form

$$(-1)^n \frac{2k_0}{\pi} \int \frac{\mathrm{e}^{\phi}}{s^2}\,\mathrm{d}s \tag{D 16}$$

for s large, where the integral is to be taken along the steepest descent path. It is straightforward to obtain the saddle point contribution using (D 15) and (D 16) as

$$\bar{M}_n \sim (-1)^n\,\mathrm{e}^{-\mathrm{i}\pi/8}\,(2k_0 L/\pi^2 n^3)^{\frac{1}{4}} \exp\left[2(\mathrm{i}-1)\,(nk_0 L)^{\frac{1}{2}}\right] \tag{D 17}$$

for $n \to \infty$. This contribution dominates that from the integral in $|s| < 2S$ and (D 17) gives the leading-order term in $\bar{M}_n$ as $n \to \infty$.

According to (D 17)

$$|\bar{M}_n|^2 \sim (2k_0 L/\pi^2 n^3)^{\frac{1}{2}} \exp\left[-4(nk_0 L)^{\frac{1}{2}}\right] \tag{D 18}$$

as $n \to \infty$. This leads directly to convergence of the series, (D 2).

References

Abrahams, I. D. 1981 Scattering of sound by heavily loaded finite elastic plate. *Proc. R. Soc. Lond.* A **378**, 89–117.

Achenbach, J. D., Gautesen, A. K. & McMaken, H. 1982 *Ray methods for waves in elastic solids.* Pitman.

Cannell, P. A. 1975 Edge scattering of aerodynamic sound by a lightly loaded elastic half-plane. *Proc. R. Soc. Lond.* A **347**, 213–238.

Cannell, P. A. 1976 Acoustic edge scattering by a heavily loaded elastic half-plane. *Proc. R. Soc. Lond.* A **350**, 71–89.

Crighton, D. G. 1979 Free and forced waves on a fluid-loaded elastic plane. *J. Sound Vib.* **63**, 225–235.

Crighton, D. G. & Innes, D. 1984 The modes, resonances and forced response of elastic structures under heavy fluid loading. *Phil. Trans. R. Soc. Lond.* A **312**, 295–341.

Gautesen, A. K. 1988*a* On the asymptotic solution to a class of integral equations. *SIAM J. appl. Math.* **48**, 294–306.

Gautesen, A. K. 1988*b* Scattering of waves by a crack: asymptotic expansion of the exact solution. *Wave Motion* **10**, 231–238.

Keogh, P. S. 1985 High-frequency scattering by a Griffith crack. 1. A crack Green-function. 2. Incident plane and cylindrical waves. *Q. Jl Mech. appl. Math.* **38**, 185–232.

Leppington, F. G. 1976 Scattering of sound waves by finite membranes and plates near resonance. *Q. Jl Mech. appl. Math.* **29**, 527–546.

Morse, P. M. & Feshbach, H. 1953 *Methods of theoretical physics.* McGraw-Hill.

Noble B. 1958 *Methods based on the Wiener–Hopf technique.* Pergamon Press.

Received 14 February 1991; accepted 21 June 1991